Observation of fractional revivals in the evolution of a Rydberg atomic wave packet

John A. Yeazell and C. R. Stroud, Jr.
University of Rochester, Institute of Optics, Rochester, New York 14627
(Received 5 November 1990; revised manuscript received 7 January 1991)

Rydberg atomic wave packets have demonstrated striking classical properties. In particular, the wave packets display regions in which they evolve like classical atoms. However, between these regions the wave packet is dispersed and its evolution departs from the classical model. In these nonclassical regions, the wave packet can either be dispersed or coalesced into a number of equally spaced sub-wave-packets. The regions in which the sub-wave-packets appear have come to be known as fractional revivals. This paper reports the observation of these fractional revivals and discusses their implications.

Observations[1,2] of the evolution of Rydberg atomic wave packets have shown that they can behave like a single particle traveling along an orbital trajectory, i.e., a classical atom. In these experiments, a radially localized wave packet was formed by the coherent excitation of Rydberg states by a short, optical pulse. The superposition state contained energy eigenstates with a range of values for the principal quantum number n with an average value of $\bar{n}$. The resulting wave packet oscillated between the inner and outer turning points of the classical orbit, and the oscillations were at the classical orbital period ($\tau_{cl}=2\pi\bar{n}^3$ a.u.). Although the short-term evolution displays a rather simple classical behavior, the long-term evolution is more complex, displaying the quantum nature of this atomic coherent state. We have previously reported[3] the observation of some of the features of this long-term evolution, particularly the decay and revival of the wave packet. Here, we examine the breakdown of the classical evolution in greater detail and report the first observation of a fractional revival.

It is the anharmonicity of the Coulomb potential that allows the quantum nature of the radial wave packet to be observed. If the Rydberg states that composed the superposition were equally spaced in energy (as in a harmonic oscillator system), the wave packet would continue with its simple classical evolution. To extend the region of classical evolution, the radial wave packet is excited so that the states in the superposition are nearly equally spaced. This is accomplished by producing a superposition with $\bar{n}$ large compared to the number of states within the superposition. However, the deviation from equal energy spacing causes the wave packet to spread slowly, and after a time the wave packet is no longer localized. Still, the classical nature is not permanently lost; we have seen that later in the evolution the wave packet revives.[3] The wave packet periodically loses and regains its classical appearance. The period of this cycle of decay and revival is $\tau_{dr}=\frac{2}{3}\pi\bar{n}^4$. This temporal behavior of the radial wave packet has been predicted in several papers.[4–10] In this paper we study in detail the region in which the atom switches from classical behavior to nonclassical behavior, and demonstrate the existence of a fractional revival in which the electron is actually split into two well-localized wave packets, each orbiting with the classical Kepler period. Both the fractional revival and the full revival are a direct result of the discrete nature of the bound atomic system.

The method for exciting the radial wave packet is straightforward. The electronic ground state of a single-electron atom interacts with a short, ultraviolet pulse and a range of np states is excited. The details of the excitation have been described in several papers.[4,5,10]

The long-term evolution of the wave packet can be seen in Fig. 1 which shows a theoretical calculation of the uncertainty product $\Delta r\Delta p_r$ as a function of time. The uncertainty product oscillates between a small value at the outer turning point and a large value at the inner turning point. It is the singularity in the potential surface that causes the wave packet to spread near the nucleus. The oscillations initially occur at the classical orbital period, but as the oscillations are damped, their period is also modified. The figure points out a region of the evolution (indicated by the dashed lines) where the wave packet is delocalized for several orbital periods and displays a wavelike character. However, the wave packet returns nearly to its original behavior (a revival) at 1.0 ns. In addition to these gross features, the figure also shows that $\Delta r\Delta p_r$ oscillates at twice the orbital frequency near 0.5 ns, and the amplitude of these oscillations indicates that the wave packet has regained some of its localization. Figure 2 shows that the doubling of the frequency is due to the splitting of the wave packet into two parts, with each part oscillating at the original frequency but 180° out of phase. This feature has been denoted a one-half fractional revival. Higher-order revivals ($\frac{1}{3},\frac{2}{7},\frac{1}{4},\ldots$) are also possible,[9] but only for a wave packet with a larger spread in n than that shown in Fig. 1.

The features of the long-term evolution can be explained by a simple argument. The short excitation pulse phases all the states in the superposition so that a single wave packet is produced. But the unequal spacing of the energy levels causes the states to get out of phase and the wave packet decays. During the one-half fractional revival, every other state in the superposition comes into

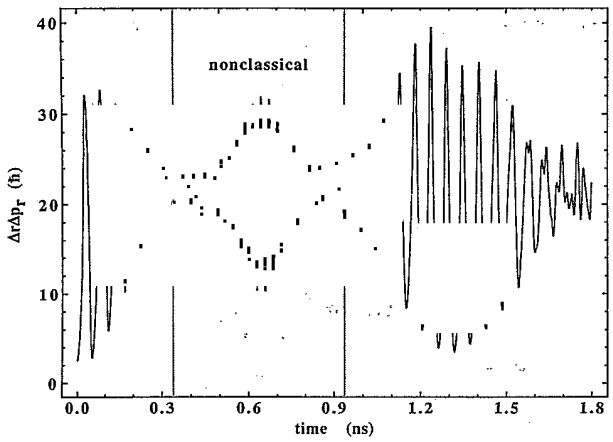

FIG. 1. The evolution of the uncertainty product of the radial wave packet. The packet has $\bar{n}=72$ and has five states significantly excited. The uncertainty product reaches a minimum as it approaches the outer turning point. Near the inner turning point the wave packet spreads and the uncertainty product reaches a maximum. The oscillations of the product are damped as the wave packet disperses. However, at approximately 1.3 ns after the exciting pulse, the oscillations have nearly regained their original amplitude. There is also a region in which the oscillations show a doubling of the frequency. This is the result of the wave packet breaking up into two distinct parts. This feature is denoted a fractional revival.

phase, leading to the formation of two wave packets. In a one-third fractional revival every third state is in phase and three sub-wave-packets are formed. Finally, at the full revival all the states are again in phase. Detailed theoretical descriptions of these fractional and full revivals have been discussed in several papers.[6–9]

The periodic motion of the wave packet produces a time dependence in the absorption cross section of the wave packet. When the wave packet is near the core, the cross section is enhanced. The wave packet is detected by probing this cross section with a short pulse at various times after the excitation of the wave packet. This pump-probe method of detecting the wave packet was first proposed by Alber, Ritsch, and Zoller.[10] Here, the probe pulse ionizes the wave packet. The features discussed previously (periodicity, decay, fractional revival, and revival) can be seen in the ion yield as a function of the probe delay.

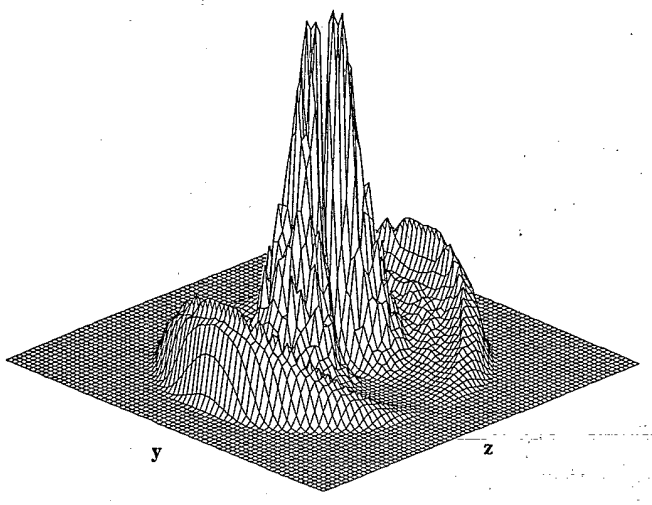

FIG. 2. A theoretical calculation of the probability density of the wave packet of Fig. 1 during the fractional revival. The y-z projection shows two sub-wave-packets, one at each extreme of the motion. The two sub-wave-packets oscillate at the classical orbital period.

This paper focuses on the evolution of the region near the fractional revival. The character of the fractional revival is a sensitive measure of the type of wave packet that has been formed. Small changes in the coherent superposition lead to large changes in the evolution near the fractional revival. This sensitivity places strict requirements on the stability of the laser system needed to observe this feature.

The excitation and detection pulses are generated in the following manner. A Quantronix 416 cw-mode-locked (76 MHz), q-switched (500 Hz) Nd:YAG (where YAG denotes yttrium aluminum garnet) laser is used to synchronously pump a dye laser. The dye laser is cavity dumped, producing pulses at the q-switch rate of the pump laser. The dye-laser pulse is 25 ps in duration full width at half maximum (FWHM) and has an energy of 10 μJ. The laser operates at approximately 5712 Å. The design of the laser is described in Ref. 2.

The output pulse of the dye laser is directed into the setup shown in Fig. 3(a). The second harmonic of the pulse is generated in the β-barium borate crystal with an efficiency of 10%. This ultraviolet pulse (2856 Å) is separated from the fundamental pulse by the dichroic mirror. The fundamental pulse enters the variable delay line. Following the delay, the fundamental pulse rejoins the path of the second harmonic pulse at another dichroic mirror. The two pulses are focused by a 20-cm focal length lens to the intersection of the optical path and the path of a thermal beam of potassium atoms. The second harmonic pulse acts as the pump and the delayed fundamental acts as the probe. A 1-m focal length lens is introduced into the delay line to assure the overlap of the focal spots of the two pulses.

Figure 3(b) depicts the interaction region and the ion-detection apparatus. The intersection of the optical and atomic beams is contained within a grounded box with ports for entrance and egress of the beams and an aperture at the top through which the photoions travel to the electron multiplier. This aperture is covered by a stainless-steel mesh which initially is held at ground. Following the optical interaction, the potential of the mesh is changed to negative 20 V. This sweeps the photoions into the electron multiplier. The signal from the electron multiplier is amplified and fed to a photon counter. After the optical interaction, the unabsorbed part of the optical pulse is directed to a 1-m Czerny-Turner spectrometer, operating in second order. The spectrum is recorded by the intensified linear detector array head of an optical multichannel analyzer. The spectrum and the output of the photon counter are transferred to a microcomputer.

The experiment proceeds as follows: The delay between the pulses is initially set to zero and then increased in steps of 3 ps. At each step, the photoion signals from 500 "good" pulses are averaged. The quality of the pulse is determined by an analysis of the spectrum of each pulse. This is the general scheme of the experiment.

One point needs to be described in greater detail. It concerns the spectral measurement of the pulse and the definition of a "good" pulse. The criteria for a good pulse are that (1) the shape is approximately Gaussian, (2) the bandwidth does not vary from 32 GHz (FWHM) by more than 20%, and (3) the center frequency of the pulse does not shift from the set frequency by more than a tenth of the bandwidth. The value for the bandwidth limit is derived from a measurement of the temporal width of the pulse. The bandwidth limit set above assures a nearly transform-limited pulse for a temporal width of 25 ps. The behavior of the wave packet during the fractional revival is strongly dependent on small changes in the frequency of the pump pulse. The spectral measurement allows strict criteria to be established for good pump pulses.

Figure 4(a) shows the ionization yield as a function of the delay time for the radially localized wave packet. The laser is tuned to produce a superposition which has $\bar{n}=72$ and $\Delta n=5$. The ion yield shows regular oscillations that slowly decay. The oscillations occur initially at the orbital period. As these oscillations are damped, the oscillations double in frequency. This doubling in frequency is characteristic of a one-half fractional revival. It is due to a splitting of the wave packet into two parts. During a fractional revival, each part approaches the nucleus during a single orbital period. The experimental results are in excellent agreement with the theoretical predictions shown in Fig. 4(b). The overall shape of the curves is the same. In particular, the positions of the peaks agree throughout the evolution. Dashed lines have been extended from some of the peaks in the theoretical plot to emphasize this agreement.

We have seen that it is possible to excite a Rydberg atom wave packet whose evolution appears classical for a

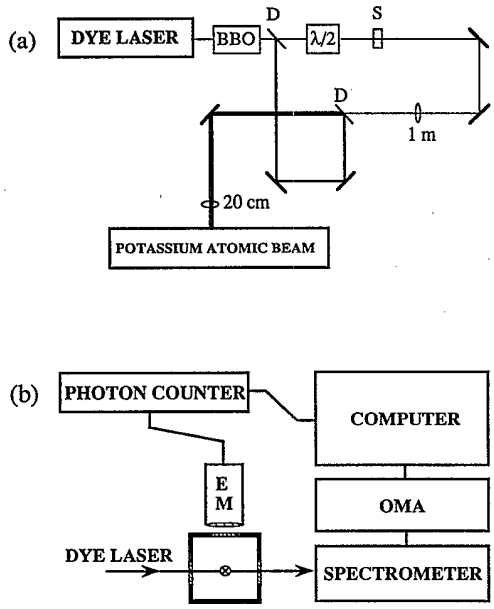

FIG. 3. The experimental apparatus. In (a) the optical layout is shown. The dye laser produces optical pulses (25 ps, 5712 Å) at a repetition rate of 500 Hz. The uv pump pulse is produced by second-harmonic generation in the BBO crystal. A dichroic mirror (D) separates the fundamental field (probe pulse) from the second-harmonic field. The probe pulse enters a delay arm, where its polarization is adjusted with a half-wave plate to match that of the pump pulse. The two pulses are recombined at a dichroic mirror and then focused onto the potassium atomic beam. A 1-m lens is introduced into the delay arm to adjust the divergence of the probe pulse. The atomic beam and detection equipment are shown in (b). The photoion signal is amplified by the electron multiplier (EM). The output of the electron multiplier is recorded by the photon counter and stored on the computer. A spectral measurement of the unabsorbed optical pulse determines whether the ion signal is accepted or rejected.

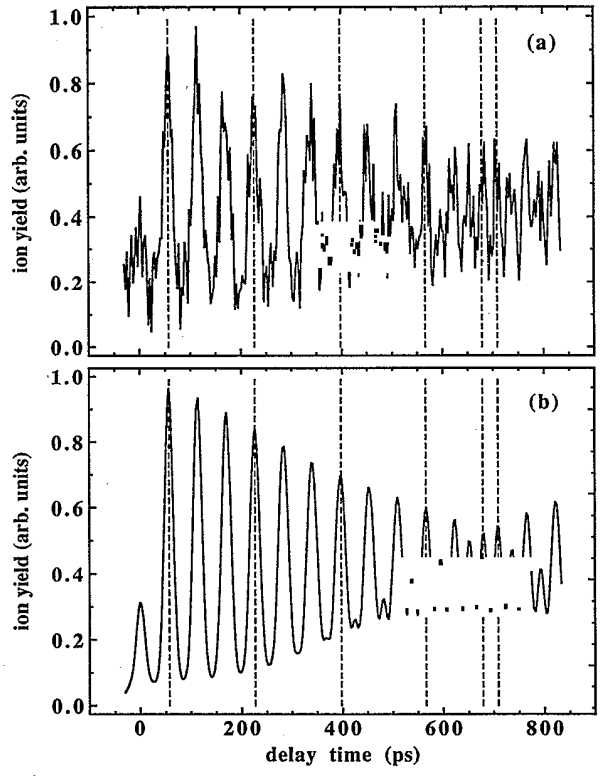

FIG. 4. The photoionization signal as a function of the delay of the probe pulse. In (a) the experimental results are shown. The signal initially oscillates at the classical orbital frequency. However, as it evolves, the oscillations change in frequency to twice the orbital frequency. The superposition was centered at $\bar{n}=72$. In (b) the theoretical prediction for the ionization signal is shown. The agreement is excellent. The dashed lines emphasize the agreement between the position of the peaks in the two curves.

time. However, we have also seen the breakdown of those simple classical orbital oscillations. This breakdown is a direct result of the quantized nature of the atom. It is the unequal spacing of the discrete energy levels of the atom that gives rise to the fractional and full revivals. This is a straightforward example of the failure of classical and semiclassical models when the quantum system is observed for an extended period of time.

To our knowledge this is the first observation of a fractional revival in any system. Decays and revivals have been observed in a Jaynes-Cummings-type atom-cavity interaction.[11] However, there have been no reports of theoretical predictions or experimental observations of fractional revivals in that system. Still, it appears that the fractional revival is a fairly general phenomenon and should be observable in other systems, such as molecules[12,13] or quantum wells.[14]

The fractional revival illustrates the complexity and subtlety of the classical limit of a single quantum system. One might expect that in this limit the quantum features of the electron would be negligibly small, showing up only in a nonzero extent of the wave packet in phase space. Indeed, this is true during some time intervals after excitation. But, inevitably, if we observe the electron over longer periods, quantum features will come to dominate the evolution. During the quantum fractional revival, the connection between the wave packet and a single classical particle orbiting the nucleus breaks down. Instead, it absorbs and emits radiation as though it were a two-peaked extended classical charge distribution moving around the orbit. One must conclude that the classical system that an atom approaches in the correspondence principle limit is not a simple massive charged point particle orbiting the nucleus, but rather a complex dynamical object following the classical orbit.

We would like to acknowledge the support of the Joint Services Optics Program and the University Research Initiative through the U.S. Army Research Office.

[1]A. ten Wolde, L. D. Noordam, H. G. Muller, A. Lagendijk, and H. B. van Linden van den Heuvell, Phys. Rev. Lett. **61**, 2099 (1988).

[2]J. A. Yeazell, M. Mallalieu, J. Parker, and C. R. Stroud, Jr., Phys. Rev. A **40**, 5040 (1989).

[3]J. A. Yeazell, M. Mallalieu, J. Parker, and C. R. Stroud, Jr., Phys. Rev. A **64**, 2007 (1990).

[4]J. Parker and C. R. Stroud, Jr., Phys. Rev. Lett. **56**, 716 (1986).

[5]J. Parker and C. R. Stroud, Jr., Phys. Scr. **T12**, 70 (1986).

[6]I. Sh. Averbukh and N. F. Perelman, Phys. Lett. **139A**, 449 (1989).

[7]M. Nauenberg, Phys. Rev. A **40**, 1133 (1989).

[8]A. ten Wolde, L. D. Noordam, H. G. Muller, and H. B. van Linden van den Heuvell, in *Fundamentals of Laser Interactions II,* edited by F. Ehlotzky (Springer-Verlag, New York, 1989).

[9]Z. D. Gaeta and C. R. Stroud, Jr., Phys. Rev. A **42**, 6308 (1990).

[10]G. Alber, H. Ritsch, and P. Zoller, Phys. Rev. A **34**, 1058 (1986).

[11]G. Rempe, H. Walther, and N. Klein, Phys. Rev. Lett. **58**, 353 (1987).

[12]R. B. Bernstein and A. H. Zewail, J. Chem. Phys. **90**, 829 (1989).

[13]R. M. Bowman, M. Dantus, and A. H. Zewail, Chem. Phys. Lett. **156**, 131 (1989).

[14]K. Leo, T. C. Damen, J. Shah, E. O. Gobel, and K. Kohler, App. Phys. Lett. **57**, 19 (1990).